HHS Public Access

Author manuscript

J Allergy Clin Immunol. Author manuscript; available in PMC 2024 August 01.

Published in final edited form as:

J Allergy Clin Immunol. 2023 August ; 152(2): 453–468. doi:10.1016/j.jaci.2023.03.027.

IgG:FcγRIIb signals block effector programs of IgE:FcεRI-activated mast cells but spare survival pathways

Cynthia Kanagaratham, PhD[1,2], **Tahereh Derakhshan, PhD**[3,4], **Yasmeen S. El Ansari, MSc**[1,5], **Kameryn N. Furiness, BS**[1], **Eleanor Hollers, BS**[3], **Mats Keldsen, BS**[1], **Hans C. Oettgen, MD, PhD**[1,2,*], **Daniel F. Dwyer, PhD**[3,4,*]

[1]Department of Pediatrics, Boston Children's Hospital, Boston, MA, 02115, USA.

[2]Department of Pediatrics, Harvard Medical School, Boston, MA, 02115, USA.

[3]Jeff and Penny Vinik Center for Allergic Disease Research, Division of Allergy and Clinical Immunology, Brigham and Women's Hospital, Boston, MA.

[4]Department of Medicine, Harvard Medical School, Boston, MA.

[5]Institute of Laboratory Medicine, Philipps University Marburg, Marburg, Germany

Abstract

Background: IgE-induced mast cell degranulation can be inhibited by IgG antibodies, signaling via FcγRIIb, but the effects of IgG on IgE-induced mast cell transcription are unknown.

Objective: Complementary transcriptomic and functional approaches were used to assess inhibitory IgG:FcγRIIb effects on mast cell responses to IgE.

Methods: RNA sequencing was performed on bone marrow-derived mast cells from wildtype and FcγRIIb-deficient mice to identify genes activated following IgE receptor crosslinking that were further modulated in the presence antigen-specific IgG in an FcγRIIb-dependent fashion. Parallel analyses of signaling pathways and allergic responses *in vivo* were performed to assess the impact of these changes in gene expression.

Results: Rapid changes in the transcription of 879 genes occurred in mast cells activated by IgE, peaking at one hour. Surprisingly, only 12% of these were altered by IgG signaling via FcγRIIb, including numerous transcripts involved in orchestrating type 2 responses linked to SYK signaling. Consistent with this finding, IgG suppressed IgE-induced phospho-intermediates in the SYK signaling pathway. *In vivo* studies confirmed that the IgG-mediated suppression of both systemic anaphylaxis and mast cell-driven tissue recruitment of inflammatory cells following

Corresponding authors: Daniel F. Dwyer, PhD, Brigham and Women's Hospital, Division of Allergy and Clinical Immunology, 60 Fenwood Road Boston, MA 02115, USA Phone: 1-617-525-1294 dfdwyer@bwh.harvard.edu, Hans Oettgen, MD, PhD Boston Children's Hospital Department of Pediatrics Division of Immunology 1 Blackfan Circle, 10213 Boston, MA 02115, USA Phone: 1-617-919-2487 hans.oettgen@childrens.harvard.edu.

*Equal contribution

All authors declare that they have no relevant conflicts of interest.

allergen challenge were dependent on FcγRIIb. In contrast, genes in the Stat5a cell survival pathway were unaltered by IgG and Stat5a phosphorylation increased after IgE-induced mast cell activation but was unaffected by IgG.

Conclusions: Our findings indicate that inhibitory IgG:FcγRIIb signals block an IgE-induced pro-allergic program but spare a pro-survival program.

Capsule Summary

IgG signaling via FcγRIIb on mast cells blocks the release of inflammatory mediators following FcεRI crosslinking but spares the pro-survival program induced by IgE-mediated mast cell activation.

Keywords

IgE; IgG; Mast Cells; FcεRI; FcγRIIb; RNA sequencing; anaphylaxis

Introduction

Mast cells (MCs) are long-lived tissue resident granulocytes thought to act as key effector cells in allergy. Their granules contain preformed mediators of hypersensitivity, including histamine, proteases and heparin (1). Antigen-induced crosslinking of IgE antibodies bound to the high-affinity IgE receptor, FcεRI, triggers the release of these granules together with rapid synthesis of pro-inflammatory eicosanoids, including prostaglandin D_2 (PGD_2) and leukotriene C_4 (LTC_4) (2). In addition to degranulation and eicosanoid production, MCs are potent sources of type 2 inflammation-linked cytokines and chemokines. While these factors play a critical role in immunity to certain pathogens, they also drive the pathophysiology of disease processes ranging from neuroinflammatory disorders to atherosclerosis (3–8).

Food allergy has emerged as a highly prevalent form of IgE-mediated hypersensitivity. While there are no curative treatments, oral immunotherapy (OIT) has emerged as a promising strategy for modulation of food allergy (9–12). A consistent feature of the immune response in subjects undergoing OIT is a multi-log increase in circulating food-specific IgG antibodies (12–18). Repertoire analysis reveals that OIT both boosts and diversifies IgG responses and that IgG specificity within individuals exhibits overlap down to the amino acid level with that of the pre-existing IgE (19). Several groups have now shown that IgG antibodies formed in response to OIT potently suppress IgE-mediated activation of MCs and basophils exposed to food allergens (18, 20–22).

Suppression of IgE-mediated MC activation by IgG is known to occur via at least two distinct mechanisms (23): epitope masking, in which IgG binds to the antigen at high enough concentrations to cover all immunodominant epitopes, effectively rendering the allergen invisible to MC-bound IgE (18), and receptor-mediated inhibition, where simultaneous engagement of an allergen by FcεRI-bound IgE and FcγRIIb -bound IgG triggers phosphatase activation and subsequent dephosphorylation of FcεRI signaling intermediates such as SYK (24, 25). We previously reported that OIT-induced IgG antibodies primarily suppress MCs via FcγRIIb receptor-mediated inhibition acting in part through blocking MC-secretion of IL-4, which suppresses regulatory T cell responses

(18, 26). Cohort studies have demonstrated that IgG antibodies arise concurrently with acquisition of food tolerance in children naturally outgrowing their food allergies, while children with higher ratios of aeroallergen specific IgG to IgE are less likely to exhibit respiratory symptoms (27, 28). Thus, IgG antibodies can both suppress allergic responses and may restore tolerance in an FcγRIIb-dependent manner.

As IgE crosslinking, in addition to eliciting MC degranulation, promotes a well-characterized pro-inflammatory MC transcriptional program (29, 30), we hypothesized that IgG engagement via FcγRIIb might suppress the gene programs induced by IgE. Using a multifaceted approach, we demonstrate that IgG:FcγRIIb signaling directly suppresses IgE:FcεRI-mediated MC degranulation, phosphorylation of SYK and downstream intermediate kinases such as ERK and p38, and induction of a select set of pro-inflammatory cytokines and chemokines. However, the vast majority of IgE-modulated transcripts, including pro-survival downstream targets of Stat5a signaling, are not impacted by IgG co-ligation, while Stat5a phosphorylation is unchanged. From these findings, we conclude that IgG signals selectively block the pro-inflammatory program of IgE-activated MCs while preserving IgE-mediated induction of Stat5aregulated genes important in MC homeostasis and cell survival.

Materials and Methods

Mouse strains

All animal studies were performed under protocols reviewed and approved by the Boston Children's Hospital Institutional Animal Care and Use Committee. Animals used in all experiments were bred and maintained in rooms and conditions that are specific pathogen-free. Animals were kept in individually ventilated cages with a maximum of five adults per cage. All mice were on the C57BL/6 background. Breeder pairs for C57BL/6 mice and FcγRIIb KO (B6;129S-FcgRIIbtm1Ttk/J) mice were purchased from The Jackson Laboratory (Bar Harbor, ME), and bred in house for experimental use. MCPT5^{Cre+} and FcγRIIb$^{fl/fl}$ mice were generously provided by Drs. Axel Roers and Sjef Verbeek respectively (31, 32). MCPT5^{Cre+} and MCPT5^{Cre+} FcγRIIb$^{fl/fl}$ mice were generated by crossing MCPT5^{Cre+} mice with FcγRIIb$^{fl/fl}$ mice. Mice were genotyped and maintained in a homozygous state. Baseline phenotyping included measurement of immunoglobulin levels, immune cell counts in peripheral blood, peritoneal cavity mast cell numbers and granularity, and assessment of FcγR expression on peritoneal cavity mast cells.

Murine mast cell culture

Murine bone marrow derived MCs (BMMCs) were cultured as previously described (33). Briefly, bone marrow cells were isolated from the femurs and tibiae of the mice. Cells were cultured with RPMI-1640 supplemented with 10% FCS (Thermo Fisher Scientific, Waltham, MA), 100 U/mL penicillin (Thermo Fisher Scientific), 100 μg/mL streptomycin (Gibco), 1% Minimum Essential Medium nonessential amino acids (Thermo Fisher Scientific), 10mM HEPES buffer (Thermo Fisher Scientific), 55μM 2-mercaptoethanol (Thermo Fisher Scientific), 10 μg/mL gentamicin (Life Technologies), and 20 ng/mL each of IL-3 and stem cell factor (SCF) (PeproTech, Thermo Fisher Scientific). Once >90% of the cells were

positive for c-KIT and FcεR1α, the concentration of cytokines was reduced to 10 ng/mL. Medium was changed weekly, and cells used in experiments were between 5 and 16 weeks old since the start of culture.

Culture of hybridomas

Hybridomas TIB141 and TIB191 were purchased from ATCC (Manassas, VA) and cells were expanded as previously described (36). The concentrations of anti-TNP IgE and anti-TNP IgG1 were determined by ELISA using commercially available reagents.

Murine LAMP-1 assay

10^5 mouse MCs in 100 uL were plated in 96 well plates. Cells were incubated overnight with anti-TNP IgE at 50 ng/mL. The following day anti-TNP IgG was added at varying concentrations (0.01–2000 μg/mL). For some experiments, non-specific IgG was used as a control at equal or greater concentrations to validate antigen-specific effect of IgG-mediated inhibition (Mouse BALB/c IgG1, clone MOPC-31C, BD Biosciences, Franklin Lakes, NJ). Fifteen minutes later, cells were stimulated with 50 ng/mL TNP-13-BSA (Biosearch Technologies, Petaluma, CA) for 10 minutes at 37°C while concurrently being stained for LAMP-1 (PE, Thermo Fisher Scientific), c-KIT (APC, Biolegend) and fixable viability dye (APC-Cy7, Thermo Fisher Scientific). Degranulation was stopped with cold FACS buffer (5% FBS in PBS with 0.1% sodium azide) and cells were pelleted by centrifuging at 1400 RPM for 5 minutes at 4°C. Cells were washed with and resuspended in FACS buffer, then acquired on an LSR Fortessa (BD Biosciences). Degranulated cells were identified as live cells that were c-KIT positive and LAMP-1 positive. Unstimulated cells were used to set the gate to identify degranulated cells.

RNA extraction, cDNA, and RT-qPCR

5×10^5 cells were cultured overnight with anti-TNP IgE in 24 well plates. Cells were treated with 10 μg/mL anti-TNP IgG then stimulated with TNP-BSA for one hour. For some experiments, non-specific IgG was used as a control at equal or greater concentrations to validate antigen-specific effect of IgG-mediated inhibition (Mouse BALB/c IgG1, clone MOPC-31C, BD). Reaction was stopped with cold PBS and cells were collected and then pelleted. Pellets were lysed with TRI reagent and RNA extraction was conducted using Direct-zol RNA mini prep kits (Zymo Research, Irvine, CA). RNA concentration was quantified using a Nanodrop 2000 (Thermo Fisher Scientific). RNA was reverse transcribed to cDNA using iScript cDNA Synthesis Kit (Biorad, Hercules, CA) following the manufacturer's instructions. qPCR was performed using Taqman Fast Advanced Mastermix (Thermo Fisher Scientific) in combination with predesigned Taqman probes (Thermo Fisher Scientific). Expression assays were performed using a QuantStudio 3 real-time qPCR instrument (Thermo Fisher Scientific). Data were analyzed using either GAPDH or HPRT as a housekeeping gene and the $2^{-\Delta\Delta Cq}$ method.

RNA-seq and Pathway analysis

Extracted RNA was processed by the Broad Institute using the low-input eukaryotic Smart-seq2 protocol as previously described (34). Data were analyzed using Bioconductor for R.

DESeq2 software was used for count normalization and differential analysis of count data (35). In comparisons between two groups, genes were considered significantly differentially expressed based on a false discovery rate of <0.1 using a Benjamini–Hochberg adjusted P value to correct for multiple comparisons. The Pheatmap software package was used to generate heatmaps. Pathway analysis was performed using the online tool Enrichr (36–38). Volcano plots were generated using the Enhanced Volcano package (42).

Flow cytometry for the detection of phosphorylated proteins

10^5 mouse MCs in 100 μL were plated in 96 well plates and incubated overnight with anti-TNP IgE. The following day, cells were treated with IgG for 15 minutes then stimulated for various time points. Cells were incubated with equal volume of Fixation buffer then permeabilized using True-Phos Permeabilization buffer (both BioLegend, San Diego, CA) following the manufacturer's instructions. Cells were stained for phosphorylated SYK (PE), ERK 1/2 (APC or FITC), p38 (PE or APC), and Stat5a (PE) at concentrations recommended by the manufacturer (all Thermo Fisher Scientific).

Detection of phosphorylated proteins by cytometry by time of flight (CyTOF)

10^5 mouse MC (FcγRIIb WT or FcγRIIb KO) were plated per well with or without 50 ng/mL anti-TNP IgE and incubated overnight to sensitize the cells. The following day the cells were washed with warm Maxpar PBS (Standard Biotools, Markham, Ontario, Canada) and stained for 5 minutes at 37°C with 5 μM Cell-ID Cisplatin Viability staining reagent according to the manufacturer's instructions (Standard Biotools). Viability dye was diluted with Maxpar PBS, washed away and cells were rested in complete media for 15 minutes at 37°C prior to proceeding. 10 ug/mL of anti-TNP IgG was added to the appropriate wells and incubated for 15 minutes at 37°C, after which cells were stimulated with 50 ng/mL of TNP-BSA for either 2 minutes or 20 minutes.

Reactions were stopped by adding equal volumes of Fixation buffer (Biolegend). Fixed cells were washed with Maxpar PBS and permeabilized with TruePhos Permeabilization buffer (Biolegend).

Permeabilized samples were incubated with palladium-based barcoding reagents according to the manufacturer's instructions (Standard Biotools). Samples were incubated in a heparin solution at 100 U/mL PBS for 15 minutes then combined into a single sample. Conjugated intracellular antibodies were added into each tube to stain phosphorylated proteins and incubated for 30 minutes. After staining, samples were fixed with 4% formaldehyde for 10 minutes. All antibodies were obtained from the Harvard Medical Area CyTOF Antibody Resource and Core (Boston, MA, USA).

The following phosphorylated proteins were measured pStat3 (Y705), pSLP-76 (S376), pSYK (Y525/526), pSHP-1 (Y564), pSTAT6 (Y641), pAKT (S473), pIRAK4 (T345/S346), pp38 (Thr180/Tyr182), p4E-BP1 (T37/46), pp90RSK (S380), pIRF-3(S396), pJAK2 (Y1008), pSTAT1 (Y701), pPLCγ1 (Tyr783), pLAT (Tyr191), and pSTAT4 (Y693). pSYK was only measured in samples stimulated for 2 minutes.

To identify single cells events, samples were labelled with 31.25uM of iridium intercalator for 20 minutes (Standard Biotools). Samples were washed and reconstituted in Maxpar Cell acquisition solution in the presence of EQ Four Element Calibration beads (Standard Biotools) at 10^6 cells/mL. Samples were acquired on a Helios CyTOF Mass Cytometer at the Longwood Medical Area CyTOF core (Boston, MA, USA). Raw FCS files were normalized, and samples were de-barcoded. Mean metal intensity (MMI) of phosphorylated proteins was obtained for each sample after gating to remove normalization beads and selecting for live single cells. Fold change in MMI (FC in MMI) was calculated for each group in each strain relative to the sensitized unstimulated group. Unscaled heatmaps of FC in MMI were generated using the Pheatmap package for R.

Flow cytometry for the detection of intracellular proteins

Expression of the anti-apoptotic protein BCL-2 was determined using BD Cytofix/Cytoperm fixation and permeabilization kit (BD Biosciences) in combination with anti-BCL2 (PE, BioLegend) as previously described (33).

Human mast cell culture

Peripheral blood was obtained from human donors at Brigham and Women's Hospital (Boston, MA). $CD34^+$ hematopoietic cells were isolated using Ficoll paque density gradient centrifugation method and magnetic cell sorting system following the manufacturer's protocol (Miltenyi Biotec, Cambridge, MA). Cells were cultured in StemSpan SFEM medium (StemCell Technologies, Vancouver, Canada) containing penicillin/streptomycin (Thermo Fisher Scientific). Differentiation of hematopoietic cells to mast cells was achieved using recombinant human IL-3 (for the first three weeks at 1 ng/mL), IL-6 (50 ng/mL), and SCF (100 μg/mL) (all PeproTech, Thermo Fisher Scientific) for 7–8 weeks with weekly media changes. Culture was deemed mature and ready to use when greater than 95% of the population was positive for c-KIT and FcεR1α.

Human LAMP-1 assay

Cells were sensitized overnight with 50 ng/mL anti-DNP IgE (SPE-7; Sigma Aldrich, St. Louis, MO). Degranulation was measured following stimulation with 50 ng/mL DNP-BSA (Bio-Techne Corporation | Tocris Biosciences, Minneapolis, MN) while simultaneously staining for LAMP-1 (PE, Biolegend) on the cells surface for one hour. Degranulation was stopped using cold FACS buffer and cells were pelleted by centrifuging for 5 minutes at 1400 RPM. Cells were then stained for c-KIT for 15 minutes at 4°C. For inhibition experiments, cells were incubated with 30 μg/mL of either anti-DNP IgG1 or IgG4 for 30 minutes (Acros Biosystems, Newark, DE). Mouse anti-CD32 clone FUN-2 (Biolegend), an antibody known to block FcγRIIb function, was used for CD32 blocking experiments (26, 39, 40). Cells were incubated with 2 μg/mL of mouse anti-CD32 for one hour prior to adding anti-DNP IgG. Cells were washed and acquired on LSR Fortessa to determine the percentage of degranulated MCs. Unstimulated cells were used to set the gate to identify degranulated cells.

Cytokine secretion from human and mouse mast cells

Human and mouse MCs were cultured with IgE, IgG and stimulated as described for LAMP-1 assays. Supernatants were collected six hours post stimulation and assayed immediately for cytokine levels by ELISA.

Passive systemic anaphylaxis

Mice were intraperitoneally injected with 2 μg of anti-TNP IgE, some mice also received 100 μg of anti-TNP IgG1. Sixteen hours post-sensitization, mice were challenged with 200 μg of TNP-BSA or PBS. Core body temperature was recorded every 5 minutes for 60 minutes via sub-dermally implanted transponders and a temperature reader (Implantable Programmable Temperature Transponder™) (Biomedic Data Systems, Seaford, DE). Negative control mice were either sensitized with PBS and challenged with TNP-BSA or sensitized with anti-TNP IgE and challenged with PBS.

Collection of peritoneal lavage fluid and staining of peritoneal lavage cells

The peritoneal cavity of mice was washed with 5 mL of cold PBS containing 10% FBS. Lavage fluid was collected, and cells were pelleted and stained for various cell subtypes. Monocytes were identified as $CD3^-$ and $CD19^-$ (AF700, Biolegend), $CD11b^+$ (BV421, Biolegend), and $F4/80^+$ (Pe-Cy7, Biolegend) live single cells. Monocytes were characterized as inflammatory if they were also positive for CCR2 and CX3CR1. Peritoneal mast cells were identified as $CD45^+$ (AF700, Biolegend), $Cd11b^-$ (FITC, Thermo Fisher Scientific), $cKIT^+$ (BV510, Biolegend) and $Fc\varepsilon RI\alpha^+$ (Pe-Cy7, Biolegend) live single cells. Lavage fluid was frozen at −20°C prior to measurement of CCL2 by ELISA.

Enzyme-Linked Immunosorbent Assays (ELISAs)

MCPT1—To detect levels of MCPT1 in the serum, mice were bled one hour following the antigen challenge. MCPT-1 was measured using the commercially available MCPT-1 ELISA kit (ThermoFisher) following the manufacturer's instructions. Cytokines in the peritoneal lavage and those secreted by BMMCs and human MCs were measured using Ready SET-Go! Kits (Thermo Fisher Scientific) following the manufacturer's instructions.

Immunoglobulin ELISAs—Immunoglobulin levels were measured by sandwich ELISAs using serum isolated from mouse blood collected retro-orbitally, or from hybridoma supernatant. ELISA plates were coated overnight with anti-mouse capture antibodies for each of the following immunoglobulins: IgG, IgG1, IgG2b, IgG3, IgA, IgE, and IgM (Southern Biotech). All capture antibodies were diluted in PBS at 2 μg/mL. The following day, plates were washed (1X PBS, 0.028% Tween) and blocked with 2% BSA-PBS for 2 hours. Samples were added at varying dilutions and incubated overnight at 4°C. Samples were detected with either HRP-conjugated detection antibodies (Southern Biotech) or biotinylated detection antibodies followed by incubation with streptavidin-HRP (R&D Systems, Minneapolis, MN). ELISAs were developed using TMB (Thermo Fisher Scientific) and reactions were stopped with 2N H_2SO_4.

Flow cytometry for the staining of Fc receptors

BMMCs and peritoneal lavage cells were stained for surface FcγRI, FcγRIIb, FcγRIII, FcγRIV or matching isotype controls for each antibody. For BMMCs, 10^5 mouse MCs in 100 uL were plated in 96 well plates and pelleted by centrifuging at 1400 RPM for 5 minutes at 4°C. Cells were resuspended in 100 uL of 2% BSA-PBS and placed at 4°C. 15 minutes later, cells were pelleted as previously described and stained for cKIT (BV510, Biolegend), FcεRIα (PE/Cy7, Biolegend), FcγRIV (BV421, Biolegend), FcγRIII (PE, Biolegend), FcγRIIb (APC, Thermo Fisher Scientific), and FcγRI (BV605, Biolegend) at 4°C for 30 minutes. Viability staining was done concurrently using the eBioscience™ Fixable Viability Dye eFluor™ 780 (Thermo Fisher Scientific). After staining, cells were pelleted before being washed with and resuspended in FACS buffer (1x PBS, 10% FBS). Peritoneal lavage was conducted as described above, and mast cells were identified as being $CD45^+$, $CD11b^-$, $cKIT^+$ and $FcεRI1α^+$. Fcγ receptor staining was done using the same antibodies as for BMMCs. Cells were acquired on an LSR Fortessa (BD Biosciences).

Statistical analysis

Results are presented as mean ± SEM of data from at least two independent experiments. Student's t test was used for pairwise comparisons, and Dunnett's multiple comparisons test was used for repeated comparisons using Prism (GraphPad Software, San Diego, CA). Unpaired t tests or ANOVA with Bonferroni post-tests was used for comparisons between unlinked groups. Two-way ANOVA followed by Tukey's multiple comparison test was used for statistical analysis of data from passive systemic anaphylaxis experiments. P values are indicated in the figures using the shorthand *P<0.05, **P<0.01, ***P<0.001, ****P<0.0001.

Results

Antigen-specific IgG inhibits mast cell degranulation in an FcγRIIb dependent manner.

The inhibitory effects of IgG antibodies on IgE-induced activation of MCs can be exerted via either epitope masking or receptor-mediated inhibition (23). In order to compare these effects and define conditions that would allow us to focus specifically on FcγRIIb-mediated effects of IgG on IgE responses, we first established a dose response of anti-TNP IgG1 inhibition of anti-TNP IgE-mediated activation of BMMC from both WT (FcγRIIb-sufficient) and FcγRIIb KO mice (41–45). As expected, antigen exposure induced strong degranulation in IgE-sensitized WT and FcγRIIb KO BMMCs compared to sensitized and unstimulated cells, as measured by surface expression of lysosomal-associated membrane protein 1 (LAMP-1) (Fig. 1A–C). IgE-sensitized unstimulated cells were used as controls to reflect the normal physiological state in allergic subjects in whom mast cells are fully saturated with IgE at rest and triggered to degranulate upon allergen exposure. Neither WT nor FcγRIIb KO BMMCs exhibited any response to exposure to IgE alone (Fig. S1). We tested the inhibition of IgE-mediated mast cell degranulation over a >5-log range of anti-TNP IgG1 concentrations (0.01 μg/mL to 2000 μg/mL) and observed a dose-responsive effect (Fig. 1A – C). Nonspecific IgG did not block LAMP-1 induction, indicating that this suppression was antigen specific (Fig. S2A). In WT BMMC, inhibition was observed starting at concentrations of 10 μg/mL with 50% inhibition of activation exerted at 40.4

μg/mL. No IgG-mediated inhibition was observed in BMMC lacking FcγRIIb below doses of 100 μg/ml and 50% inhibition required 1149 μg/mL IgG, indicating a 28.4-fold higher IgG requirement for epitope masking relative to receptor mediated inhibition. We noted that, compared to WT BMMCs, KO BMMCs exhibited a greater maximal percentage of degranulation (Fig.1B). We speculate that, since KO BMMCs have higher levels of FcγRIII than the WT BMMCs (Fig. S3A and B), they might have an increased cellular pool of the activating protein tyrosine kinases that mediate mast cell activation by both FcεRI. In addition, in conditions where antigen specific IgG is present, activating Fcγ receptors may exert a positive effect. Our findings establish that, at 10 μg/mL, IgG-mediated inhibition of IgE signaling is mediated exclusively by FcγRIIb and we thus selected that dose for subsequent investigations of IgG:FcγRIIb effects IgE-induced responses in BMMCs.

Antigen:IgE stimulation of BMMCs induces a rapid transcriptional response that is partially suppressed by IgG antibodies signaling via FcγRIIb.

A time course analysis was first performed to determine the optimal time at which to interrogate the inhibitory effects of IgG on the MC transcriptome. RT-qPCR was used to analyze a panel of cytokine transcripts known to be regulated by IgE (*Il4*, *Il6*, *Il13, Tnfa*), *Hdc*, encoding histidine decarboxylase, a critical component of histamine biosynthesis, and eicosanoid biosynthetic enzymes (*Alox5, Alox5ap, Ltc4s, Ptgs2*). While expression of *Alox5*, *Alox5ap*, and *Ltc4s* did not change following stimulation, the remaining genes exhibited similar kinetics with rapid upregulation peaking at one hour (Fig. 1D). To compare the relative impacts of epitope masking and receptor-mediated inhibition on MC transcription at this dosage and timepoint, we evaluated *Il13* expression in both WT and FcγRIIb KO BMMCs. While 10 μg/mL IgG significantly inhibited IgE-mediated *Il13* upregulation in WT BMMCs, no such effect was evident in the FcγRIIb KO BMMCs (Fig. 1E). Inhibition of *Il4* and *Il13* expression by 50% was observed in the KO BMMCs at IgG concentrations of 674 μg/mL and 415 ug/mL, respectively (Fig. S4A and B). Interestingly, FcγRIIb KO BMMCs trended towards increased activation at IgG doses lower than 10 μg/mL, a phenomenon that might relate to their increased expression of the activating IgG receptor, FcγRIII. In WT BMMCs, a dose of only 0.1 ug/mL of IgG was sufficient to observe 50% inhibition of *Il4* expression (Fig. S4C), while 6 ug/mL was sufficient for *Il13* (Fig. S4D). Nonspecific IgG had no effect under these conditions (Fig. S2). Thus, in addition to suppressing degranulation, FcγRIIb engagement had a direct impact on MC upregulation of select pro-inflammatory mediators in response to IgE.

IgE crosslinking upregulates proinflammatory and survival pathways in mast cells.

To determine if FcγRIIb signaling has a global impact on the IgE induced transcriptome or affects only select pathways, we conducted RNA sequencing on anti-TNP IgE-sensitized WT and FcγRIIb KO BMMCs cells treated with or without 10 μg/mL of anti-TNP IgG and challenged with TNP-BSA or vehicle. Transcriptional analysis of IgE-stimulated WT BMMCs compared to unstimulated WT BMMCs identified 879 genes that were differentially expressed, with 530 genes upregulated and 349 genes downregulated one hour after IgE receptor crosslinking (Fig. 2A and B, Table S1). Consistent with prior reports (46), IgE crosslinking upregulated transcripts for numerous cytokines, chemokines, and growth factors including the classical MC cytokines *Il4*, *Il13*, and *Tnfa*, members of the

Il6 family (*Il6*, *Lif* and *Osm*) and the chemokines *Ccl1*, *Ccl2*, *Ccl3*, *Ccl4*, and *Ccl9* (Fig. 2C). We further noted upregulation of a range of growth factors and survival associated transcripts (Fig. 2C). Many of the induced transcripts are targets of the SYK signaling pathway (47). Consistent with this, we observed an increase in phosphorylation of SYK, ERK, and p38 signaling intermediates as measured by flow cytometry after IgE receptor crosslinking (Fig. 2D–F). Pathway analysis of RNAseq results indicated enrichment for several additional pathways following activation, including Stat5a signaling targets (Table S2), a category that included multiple pro-survival transcripts (Fig. 2C). Consistent with this finding, Stat5a phosphorylation was similarly observed following FcεRI crosslinking (Fig. 2G). Taken together, our results establish that FcεRI crosslinking leads to rapid changes in gene expression.

Antigen-specific IgG signals affect only a small fraction of transcripts altered following IgE-mediated mast cell activation.

To assess the effects of IgG:FcγRIIb inhibition on the IgE-modulated transcriptome, we examined the responses of IgG-treated WT and FcγRIIb-deficient MCs. As anticipated, principal component analysis showed clear separation between BMMCs activated by IgE crosslinking and sham stimulation in both WT and KO BMMCs and suggested an additional effect of IgG co-ligation in IgE-activated WT BMMCs (Fig. 3A). As separation was also observed between FcγRIIb WT and KO BMMCs under all conditions (indicating inherent differences in the transcriptome of BMMCs from the two strains), analysis of FcγRIIb KO BMMCs was restricted to IgE-responsive genes for all subsequent comparisons. Direct comparison of WT cells activated through IgE crosslinking versus IgE and IgG co-ligation indicated that only 128 genes were differentially regulated between the two conditions, of which 108 were among the 879 genes differentially regulated in MCs following IgE crosslinking (Fig. 3B, Table S3). In FcγRIIb KO BMMCs, IgE receptor crosslinking induced changes in 645 genes compared to unstimulated cells (Fig. S5). While 166 transcripts were differentially regulated between the IgE-stimulated KO BMMCs and IgE and IgG co-stimulated KO BMMCs, these did not overlap with the 128 genes affected in the WT cells (Fig. S5).

Of the 108 IgE crosslinking target genes impacted by IgG co-ligation, 88 genes were upregulated following IgE receptor crosslinking but diminished with IgG co-ligation while 20 were downregulated following IgE receptor crosslinking but enhanced by IgG co-ligation (Fig. 3C, left panel). This cassette of 108 genes was predominantly unchanged by IgG ligation in FcγRIIb KO BMMCs, indicating that the IgG-mediated transcriptional effects were the result of receptor-mediated inhibition acting via FcγRIIb (Fig. 3C right panel). IgG cross-linking in the absence of IgE had minimal impact on WT BMMCs at the time point and concentration assessed (Fig. S5D).

Antigen-specific IgG signaling via FcγRIIb inhibits phosphorylation of SYK and its downstream signaling intermediates, and secretion of cytokines and chemokines.

The phosphorylation of the immunoreceptor tyrosine-based activation motifs (ITAMs) in FcεRI generates docking sites for SYK tyrosine kinase, and phosphorylation of SYK by Lyn leads to subsequent phosphorylation of downstream mediators such as ERK and p38 (47).

Following IgE crosslinking, SYK, ERK and p38 exhibited rapid phosphorylation that was quickly suppressed by IgG co-ligation, with IgG nearly abolishing phosphorylation of SYK by two minutes, and ERK and p38 by 20 minutes (Fig. 4A). In contrast, IgG ligation in the absence of IgE failed to affect phosphorylation of these kinases in KO BMMCs (Fig. 4A). These findings indicate that the dephosphorylated state of these intermediates in WT BMMCs is maintained by activation of FcγRIIb. Genes, such as *Ccl2*, *Il6*, *Il13* and *Tnfa*, identified as downstream of SYK and its signaling intermediates by pathway analysis, were inhibited by IgG co-ligation (Fig. 4B, Table S3). Consistent with our transcriptomics results, we found that IgG co-ligation inhibited IgE-mediated protein secretion of CCL2, IL6, IL13 and TNF-α from WT BMMCs (Fig. 4C). In contrast, IgG-treated FcγRIIb-deficient BMMCs, exhibited increased CCL2, IL-13 and TNF- α secretion but no difference in IL-6 secretion (Fig. 4C). The increase in cytokine production induced by IgE in the FcγRIIb-deficient BMMC may be due to their elevated levels of activating FcγRIII expression (Fig. S3).

To further determine the effects of IgG on IgE-driven phosphorylation of signaling intermediates, we utilized cytometry by time of flight (CyTOF) to evaluate 17 additional protein phosphorylation events. We stimulated BMMCs from each genotype for 2 and 20 minutes to assess early and late phosphorylation following IgE receptor crosslinking (Fig. 4D, Fig. S7 and S8). We observed an increase in phosphorylation of members of the SYK pathway, including SYK, AKT, SLP-76, LAT, PLCα1, p38, and p90RSK by 2 minutes (Fig. 4D and S7A–G). In the presence of IgG, IgE-mediated phosphorylation was inhibited in most of the above following 2 minutes of stimulation while inhibition of AKT phosphorylation was observed at 20 minutes. None of these IgE-mediated phosphorylation events were inhibited in the FcγRIIb KO cells in the presence of IgG.

In addition to these SYK pathway intermediates, we observed that a number of STAT molecules (STAT1, STAT3, STAT4, STAT6) and JAK2 were phosphorylated following IgE receptor crosslinking in the FcγRIIb WT cells at both 2 and 20 minutes of stimulation (Fig. S6, S7H–L, S8G–K). In addition, phosphorylation was observed for IRAK4, 4E-BP1, IRF-3 and SHP-1 at 2 minutes (Fig S6, S7M–P). While most phosphorylation events were reduced in the presence of IgG after 20 minutes in WT cells, phosphorylated forms of STAT3, JAK2, and IRAK-4, persisted (Fig. S8H, K and L, respectively). No inhibition in IgE-mediated phosphorylation of any of these proteins was observed in FcγRIIb KO cells. This is consistent with our phosphoprotein flow cytometry findings demonstrating that IgE-induced phosphorylation of many signaling intermediates, including members of the SYK pathway, is suppressed by IgG in an FcγRIIb-dependent manner. Additionally, a subset of proteins with persistent phosphorylation irrespective of the presence of antigen specific IgG was identified.

Antigen-specific IgG blocks the degranulation of human mast cells in a CD32 dependent manner.

In order to extend our analysis to human MCs, we used peripheral blood-derived MCs. After confirming expression of both FcγRIIa/b (CD32) and FcεRI on human MCs (Fig. 5A, 5B and S9), we sensitized the cells with anti-DNP IgE and incubated the cells with

either anti-DNP IgG1, an isotype that has sometimes been considered to act primarily through receptor-mediated inhibition, or anti-DNP IgG4, thought to act primarily through epitope masking (48). Incubation of sensitized cells with either IgG isotype prior to simulation with DNP-BSA blocked degranulation (Fig. 5C) and CCL2 secretion (Fig. 5D) to a similar extent. Interestingly, inhibiting IgG receptor binding by pre-incubation with anti-CD32 fully negated the inhibitory effects of both IgG1 and IgG4 on degranulation and CCL2 production. This implicated FcγRIIb receptor-mediated inhibition rather than epitope masking as the dominant inhibitory mechanism mediating both IgG1 and IgG4 effects at this IgG concentration. To further explore the effects of IgG4:FcγRIIb on human MCs, we assessed phosphorylation of the signaling intermediate ERK following IgE receptor crosslinking, observing significant inhibition by IgG4 in an FcγRIIb dependent manner (Fig. 5E). Thus, as with IgG1: FcγRIIb in mouse, the selective impact of IgG4:FcγRIIb engagement on the human MC transcriptional response to IgE crosslinking appeared to be related in part to regulation of SYK target protein phosphorylation states.

Antigen-specific IgG blocks neither the phosphorylation of Stat5a nor changes in Stat5a-associated transcripts in BMMCs induced by IgE receptor crosslinking.

The observation that only a subset of IgE-target transcripts was affected by IgG indicated that signaling pathways activated by FcεRI crosslinking may have differential sensitivity to suppression by IgG. Pathway analysis identified the Stat5a gene module that includes transcript encoding the survival factor BCL2 (*Bcl2*) as resistant to suppression by IgG (Fig. 6A). Further analysis of the BCL2 family indicated IgE-mediated downregulation of the pro-apoptotic factor Bid and upregulation transcripts encoding the anti-apoptotic factors MCL1 (*Mcl1)* and BCL2 (*Bcl2*) were all unaffected by IgG co-ligation (Fig. 6A and B). These findings led us to consider that Stat5a phosphorylation and subsequent induction of anti-apoptotic factors might be resistant to the phosphatases activated by FcγRIIb. Flow cytometric analysis confirmed robust Stat5a phosphorylation following IgE crosslinking, that was unaffected by IgG in both WT and FcγRIIb KO BMMCs (Fig. 6C). We observed that deprivation of the BMMC survival-sustaining cytokines IL-3 and SCF decreased BCL2 expression and that IgE receptor crosslinking (in the absence of survival cytokines) increased it (Fig. 6D), as previously described by others (49). As predicted by both RNASeq analysis and Stat5a phosphorylation, intracellular BCL2 induction following IgE crosslinking was unaffected by IgG co-ligation (Fig. 6E). Overall, our data demonstrate that IgG suppresses induction of inflammatory mediators by IgE but does not impair IgE-induced activation of Stat5a and downstream pro-survival pathways.

Antigen-specific IgG blocks IgE-mediated anaphylaxis and the recruitment of inflammatory cells.

Our findings in both mouse and human align with the concept that, in addition to being effector cells of immediate hypersensitivity, MCs are a source of pro-inflammatory chemokines that could recruit myeloid cells to inflammatory sites and that FcγRIIb might inhibit these functions. To test this hypothesis *in vivo*, we generated a lineage specific deletion of FcγRIIb in MCs by crossing MCPT5^{Cre+} mice with FcγRIIb$^{fl/fl}$ mice (31, 32). FcγR expression was assessed on peritoneal cavity mast cells, confirming mast cell restricted FcγRIIb deletion but also indicating FcγRIII upregulation in

MCPT5^{Cre+}FcγRIIb$^{fl/fl}$ mice (Fig. S10A), similar to that observed in BMMCs derived from FcγRIIb germline KO mice (Fig. S3). We confirmed that FcγRIIb expression remained intact on B cells and basophils from MCPT5^{Cre+}FcγRIIb$^{fl/fl}$ mice as a control against unintentional germline deletion of FcγRIIb (Fig. S10B). No differences were observed in peritoneal cavity MC numbers or granularity (Fig. S10C–D). At baseline, MCPT5^{Cre+}FcγRIIb$^{fl/fl}$ mice had higher serum levels of total IgG1 than their MCPT5^{Cre+} counterparts.

The impact of MC-specific FcγRIIb deletion on IgE-mediated immediate hypersensitivity was next tested using a model of passive systemic anaphylaxis in MCPT5^{Cre+}FcγRIIb$^{fl/fl}$ mice relative to MCPT5^{Cre+} littermate controls. No change in core body temperature was observed for mice either sensitized with anti-TNP IgE and challenged with PBS or sensitized with PBS and challenged with TNP-BSA (Fig. 7A), while both MCPT5^{Cre+} controls and MCPT5^{Cre+} FcγRIIb$^{fl/fl}$ animals sensitized with anti-TNP IgE and challenged with TNP-BSA exhibited a significant drop in core body temperature when compared to their respective anti-TNP IgE sensitized and PBS challenged controls, indicative of systemic anaphylaxis (p <0.0001 for both, detailed statistical analysis are in Table S4). In MCPT5^{Cre+} animals, co-sensitization with anti-TNP IgE and anti-TNP IgG attenuated anaphylaxis, while this attenuation not observed in MCPT5^{Cre+} FcγRIIb$^{fl/fl}$ animals. These observations confirmed a direct role for FcγRIIb in IgG inhibition of MC activation *in vivo*, consistent with prior studies using mice with germline deletion of FcγRIIb (26). Plasma levels of the MC granule protease MCPT-1, a marker of MC degranulation, correlated with the physiological responses. IgG-mediated suppression of IgE-induced MCPT-1 release was evident only in MCPT5^{Cre+} control mice (Fig. 7B).

Our transcriptomic data as well as published studies reveal that MCs are prolific producers of chemokine ligands following IgE crosslinking, including *Ccl1*, *Ccl2*, *Ccl3*, and *Ccl4* (Fig. 7C) (30). All of these were suppressed by IgG co-administration in WT but not FcγRIIb KO BMMCs (Fig. 3C). To determine the relevance of this anti-inflammatory IgG:FcγRIIb axis *in vivo*, CCL2 was measured in peritoneal lavage fluid six hours following antigen challenge of passively IgE sensitized mice. Consistent with our prior observations in cultured BMMC, CCL2 levels were increased in the peritoneal lavage of MCPT5^{Cre+} mice following challenge but were significantly inhibited in mice that also received IgG, a protective effect that was absent in IgG-treated MCPT5^{Cre+} FcγRIIb$^{fl/fl}$ mice (Fig. 7D). Chemokines produced by MCs following IgE crosslinking are involved in the recruitment of a variety of cell types, including monocytes (50). To test if peritoneal MC activation under these conditions would trigger leukocyte recruitment and whether IgG might modulate this effect, we measured peritoneal monocyte numbers following IgE (±IgG) sensitization and allergen challenge. IgE-sensitized and challenged animals exhibited a marked increase in peritoneal CCR2^{+}CX3CR1^{+} inflammatory monocytes. Treatment with IgG blocked the recruitment of these cells in the MCPT5^{Cre+} mice, while the appearance of these cells in IgG-treated MCPT5^{Cre+} FcγRIIb$^{fl/fl}$ mice was unimpaired (Fig. 7E). Together, these findings identify activated MCs as a source of CCL2 *in vivo*, demonstrate that IgG:FcγRIIb engagement dampens the production of pro-inflammatory chemokines elicited upon MC activation by IgE, and specifically implicate the IgG:FcγRIIb signaling axis as an important regulator of effector cell recruitment and inflammation orchestrated by IgE-activated MCs.

Discussion

MCs are well known inducers of rapid allergic reactions, including anaphylaxis, which occurs following crosslinking of allergen-specific IgE antibodies bound to FcεRI. Activation in this manner leads to immediate release of preformed mediators contained in granules, rapid eicosanoid synthesis, and *de novo* generation of cytokines and chemokines within hours. Here, we define mechanisms whereby the inhibitory IgG receptor FcγRIIb selectively regulates these MC responses. FcγRIIb co-ligation potently inhibits degranulation and pro-inflammatory protein synthesis following IgE crosslinking both *in vitro* and *in vivo*. Deletion of FcγRIIb in mast cells *in vivo* negates the protective effects of IgG in IgE-mediated passive systemic anaphylaxis and in mast cell driven inflammatory cell recruitment. Together with our observations that FcγRIIb co-ligation is nearly 30-fold more potent than epitope masking in inhibiting MC degranulation, these findings establish a dominant role for receptor-mediated inhibitory signals over a “blocking” effect of IgG antibodies on antigenic epitopes.

The mechanisms of FcγRIIb mediated suppression have been extensively characterized by others. Following ligand binding and aggregation with an activating receptor such as FcεRI, tyrosine residues in the immunoreceptor tyrosine-based inhibitory motif (ITIM) of FcγRIIb are phosphorylated by Lyn (51), providing docking sites for Src homology 2 (SH2) domain-containing protein tyrosine phosphatases (SHPs) as well as inositol phosphatases (SHIPs). SHP-1 has been shown to dephosphorylate several early molecules in FcεRI signal transduction pathway, including SYK, LAT, and SLP76 (52, 53), while SHIP-1 acts to hydrolyze phosphatidylinositol (3,4,5)-trisphosphate necessary for calcium flux and degranulation in mast cells (54). These mechanisms may provide clues for our observation of enhanced cytokine secretion by IgE stimulated FcγRIIb-deficient MC (Figs. 1E, 4C). We find that, in the absence of FcγRIIb, transcript encoding SHP-1 (*Ptpn6*) is significantly decreased, which we speculate might result in an overall decrease in MC inhibitory tone (Fig. S5E). Similarly, the further increase in cytokine production by IgE-stimulated FcγRIIb KO BMMCs occurring following the addition of IgG to the cultures may reflect a dominant activating effect mediated by FcγRIII (whose expression is increased, Fig. S3) in cells lacking FcγRIIb.

The FcγRIIb mediated suppressive effects of allergen-specific IgG antibodies observed *in vitro* were recapitulated in our *in vivo* passive systemic anaphylaxis model, where we observed significant suppression of antigen:IgE-induced hypothermia in control MCPT5^{Cre+} mice but not in MCPT5^{Cre+}FcγRIIb$^{fl/fl}$ animals (Fig 7A, Table S4). Our finding that, under the conditions studied, most of the suppressive effect of IgG was exerted by inhibitory signaling via FcγRIIb rather than epitope masking align well with prior reports showing increased anaphylaxis in mice with germline deletion of FcγRIIb (26, 55). However, Strait *et al* found that at high concentrations of IgG and antigen, inhibition of IgE mediated activation occurs predominately by epitope masking, suggesting that the inhibitory potential of IgG via FγRIIb might be more relevant at limiting concentrations of IgG (56). Observations by Strait *et al* regarding high dose-IgG align with our *in vitro* observations that high concentrations of IgG attenuate IgE mediated activation even in mast cells lacking FcγRIIb (Fig 1). Taken together, our findings along with those of other groups indicate that

this is a complex biological system whose signaling outcomes can be significantly affected by the stoichiometry of IgE:IgG:antigen and FcγR interactions.

In contrast to its pronounced effects on MC degranulation, the impact of IgG on transcriptional responses was more nuanced. We find that IgE cross-linking rapidly induces changes in 879 genes, of which only 108 are inhibited by FcγRIIb co-ligation. Many of the inhibited transcripts are SYK signaling targets, and consistent with this we find FcγRIIb co-ligation rapidly suppresses phosphorylation of SYK pathway signaling intermediates. *In vivo*, we observe that FcγRIIb co-ligation suppresses MC IgE-driven CCL2 secretion and resultant monocyte recruitment in addition to protecting from anaphylaxis. In contrast, IgE-elicited Stat5a phosphorylation and the subsequent induction of survival genes previously identified as Stat5a targets is not inhibited by IgG:FcγRIIb.

While prior studies have demonstrated IgG-FcγRIIb receptor-mediated inhibition of IgE-triggered MC degranulation (18, 26), here we find that IgG:FcγRIIb additionally exerts a selective inhibitory effect on FcεRI induced genes. While FcγRIIb co-ligation impacted only 12% of FcεRI crosslinking target genes, these transcripts include potent immunoregulatory cytokines, chemokines, and growth factors. Our findings are consistent with a focused role for IgG in modulating MC-driven inflammation but not impacting MC homeostasis, supporting the concept of IgG acting as a humoral “off switch” for IgE-induced pro-inflammatory MC responses.

In contrast to cytokine and chemokine-encoding genes, BCL2 family member transcripts were resistant to IgG co-ligation, which pathway analysis linked to Stat5a. While our studies did not address the impact of epitope masking on this pro-survival pathway, we speculate it would block Stat5a phosphorylation, creating an interesting point of divergence between epitope masking and receptor-mediated inhibition. The role of Stat5a in MC biology has previously been extensively explored by Ryan and colleagues, who similarly observed that FcεRI crosslinking elicits Stat5a phosphorylation and further found that MCs cultured from Stat5a deficient mice exhibit decreased survival and impaired proliferation (57–60). Stat5a deficient BMMCs have been found to have decreased Bcl-2 expression (58, 61). Our data further demonstrate that, unlike SYK and its signaling intermediates, Stat5a phosphorylation is not inhibited by FcγRIIb. This may be because de-phosphorylation of Stat5a is not dependent on SHP-1 phosphatases.

These findings have potential clinical implications. IgG antibodies have recently been introduced into clinical practice in the care of respiratory allergy. Orengo and colleagues have shown that cocktails of monoclonal IgG antibodies to Fel d 1 suppress symptoms in cat allergic subjects, while Bet v 1 IgG4 reduced rhinitis in those with birch allergy (48, 62). Our results additionally suggest that inhibitory IgG antibodies might offer a beneficial adjuvant effect for allergen immunotherapy, modulating immune responses via FcγRIIb at much lower doses than would be required to achieve epitope masking. Thus, it will be critical to assess the mechanistic effects of IgG therapies on both established and emerging adaptive immune responses as well as allergic inflammation in these disease settings.

Supplementary Material

Refer to Web version on PubMed Central for supplementary material.

Acknowledgments

We thank Dr. Axel Roers for MCPT5^{Cre+} mice (A-Mcpt5-Cre, Tg$^{Mcpt5\text{-}Cre}$) and Dr. Sjef Verbeek for FcγRIIb$^{fl/fl}$ (FcgammaRIIB^{fl}, FcgammaRIIB^{Flox}, Fcgr2b$^{tm1.1Sjv}$). We thank the laboratory of Dr. Jim Lederer at Brigham and Women's Hospital for advice on conducting CyTOF experiment.

Funding sources:

D.F. Dwyer was supported by National Institutes of Health grant K22 AI146281 and by the Brigham and Womens' Hospital Department of Medicine Hearst Young Investigator award. H.C. Oettgen was supported by National Institutes of Health grant 2R01AI119918-06 and the Food Allergy Science Initiative. C. Kanagaratham was supported by postdoctoral training awards from the Fonds de recherche Québec – Santé (258617 and 285834).

Abbreviations:

MC	mast cell
OIT	oral immunotherapy
IL	interleukin
CCL	chemokine ligand
MCPT-1	mast cell protease −1
LAMP-1	lysosomal associated membrane protein – 1
IgE	immunoglobulin E
IgG	immunoglobulin G

References

1. Galli SJ. The Mast Cell-IgE Paradox: From Homeostasis to Anaphylaxis. Am J Pathol. 2016;186(2):212–24. [PubMed: 26776074]
2. Boyce JA. Mast cells: beyond IgE. J Allergy Clin Immunol. 2003;111(1):24–32; quiz 3. [PubMed: 12532090]
3. Huang C, Friend DS, Qiu WT, Wong GW, Morales G, Hunt J, et al. Induction of a selective and persistent extravasation of neutrophils into the peritoneal cavity by tryptase mouse mast cell protease 6. J Immunol. 1998;160(4):1910–9. [PubMed: 9469453]
4. Biedermann T, Kneilling M, Mailhammer R, Maier K, Sander CA, Kollias G, et al. Mast cells control neutrophil recruitment during T cell-mediated delayed-type hypersensitivity reactions through tumor necrosis factor and macrophage inflammatory protein 2. J Exp Med. 2000;192(10):1441–52. [PubMed: 11085746]
5. Galli SJ, Nakae S, Tsai M. Mast cells in the development of adaptive immune responses. Nat Immunol. 2005;6(2):135–42. [PubMed: 15662442]
6. Gregory GD, Raju SS, Winandy S, Brown MA. Mast cell IL-4 expression is regulated by Ikaros and influences encephalitogenic Th1 responses in EAE. J Clin Invest. 2006;116(5):1327–36. [PubMed: 16628252]
7. Abraham SN, St John AL. Mast cell-orchestrated immunity to pathogens. Nat Rev Immunol. 2010;10(6):440–52. [PubMed: 20498670]

8. Wang J, Cheng X, Xiang MX, Alanne-Kinnunen M, Wang JA, Chen H, et al. IgE stimulates human and mouse arterial cell apoptosis and cytokine expression and promotes atherogenesis in Apoe−/− mice. J Clin Invest. 2011;121(9):3564–77. [PubMed: 21821913]
9. Brozek JL, Terracciano L, Hsu J, Kreis J, Compalati E, Santesso N, et al. Oral immunotherapy for IgE-mediated cow's milk allergy: a systematic review and meta-analysis. Clin Exp Allergy. 2012;42(3):363–74. [PubMed: 22356141]
10. Burks AW, Jones SM, Wood RA, Fleischer DM, Sicherer SH, Lindblad RW, et al. Oral immunotherapy for treatment of egg allergy in children. N Engl J Med. 2012;367(3):233–43. [PubMed: 22808958]
11. Fleischer DM, Burks AW, Vickery BP, Scurlock AM, Wood RA, Jones SM, et al. Sublingual immunotherapy for peanut allergy: a randomized, double-blind, placebo-controlled multicenter trial. J Allergy Clin Immunol. 2013;131(1):119–27 e1–7. [PubMed: 23265698]
12. Vickery BP, Lin J, Kulis M, Fu Z, Steele PH, Jones SM, et al. Peanut oral immunotherapy modifies IgE and IgG4 responses to major peanut allergens. J Allergy Clin Immunol. 2013;131(1):128–34 e1–3. [PubMed: 23199605]
13. Jones SM, Pons L, Roberts JL, Scurlock AM, Perry TT, Kulis M, et al. Clinical efficacy and immune regulation with peanut oral immunotherapy. J Allergy Clin Immunol. 2009;124(2):292–300, e1–97. [PubMed: 19577283]
14. Vickery BP, Pons L, Kulis M, Steele P, Jones SM, Burks AW. Individualized IgE-based dosing of egg oral immunotherapy and the development of tolerance. Ann Allergy Asthma Immunol. 2010;105(6):444–50. [PubMed: 21130382]
15. Kim EH, Bird JA, Kulis M, Laubach S, Pons L, Shreffler W, et al. Sublingual immunotherapy for peanut allergy: clinical and immunologic evidence of desensitization. J Allergy Clin Immunol. 2011;127(3):640–6 e1. [PubMed: 21281959]
16. Bedoret D, Singh AK, Shaw V, Hoyte EG, Hamilton R, DeKruyff RH, et al. Changes in antigen-specific T-cell number and function during oral desensitization in cow's milk allergy enabled with omalizumab. Mucosal Immunol. 2012;5(3):267–76. [PubMed: 22318492]
17. Schneider LC, Rachid R, LeBovidge J, Blood E, Mittal M, Umetsu DT. A pilot study of omalizumab to facilitate rapid oral desensitization in high-risk peanut-allergic patients. J Allergy Clin Immunol. 2013;132(6):1368–74. [PubMed: 24176117]
18. Burton OT, Logsdon SL, Zhou JS, Medina-Tamayo J, Abdel-Gadir A, Noval Rivas M, et al. Oral immunotherapy induces IgG antibodies that act through FcgammaRIIb to suppress IgE-mediated hypersensitivity. J Allergy Clin Immunol. 2014;134(6):1310–7 e6. [PubMed: 25042981]
19. Chen G, Shrock EL, Li MZ, Spergel JM, Nadeau KC, Pongracic JA, et al. High-resolution epitope mapping by AllerScan reveals relationships between IgE and IgG repertoires during peanut oral immunotherapy. Cell Rep Med. 2021;2(10):100410. [PubMed: 34755130]
20. Santos AF, James LK, Bahnson HT, Shamji MH, Couto-Francisco NC, Islam S, et al. IgG4 inhibits peanut-induced basophil and mast cell activation in peanut-tolerant children sensitized to peanut major allergens. J Allergy Clin Immunol. 2015;135(5):1249–56. [PubMed: 25670011]
21. Santos AF, James LK, Kwok M, McKendry RT, Anagnostou K, Clark AT, et al. Peanut oral immunotherapy induces blocking antibodies but does not change the functional characteristics of peanut-specific IgE. J Allergy Clin Immunol. 2020;145(1):440–3 e5. [PubMed: 31676085]
22. Sampath V, Abrams EM, Adlou B, Akdis C, Akdis M, Brough HA, et al. Food allergy across the globe. J Allergy Clin Immunol. 2021;148(6):1347–64. [PubMed: 34872649]
23. Daeron M, Malbec O, Latour S, Arock M, Fridman WH. Regulation of high-affinity IgE receptor-mediated mast cell activation by murine low-affinity IgG receptors. J Clin Invest. 1995;95(2):577–85. [PubMed: 7860741]
24. Smith KG, Clatworthy MR. FcgammaRIIB in autoimmunity and infection: evolutionary and therapeutic implications. Nat Rev Immunol. 2010;10(5):328–43. [PubMed: 20414206]
25. Kanagaratham C, El Ansari YS, Lewis OL, Oettgen HC. IgE and IgG Antibodies as Regulators of Mast Cell and Basophil Functions in Food Allergy. Front Immunol. 2020;11:603050. [PubMed: 33362785]

26. Burton OT, Tamayo JM, Stranks AJ, Koleoglou KJ, Oettgen HC. Allergen-specific IgG antibody signaling through FcgammaRIIb promotes food tolerance. J Allergy Clin Immunol. 2018;141(1):189–201 e3. [PubMed: 28479335]
27. Caubet JC, Bencharitiwong R, Moshier E, Godbold JH, Sampson HA, Nowak-Wegrzyn A. Significance of ovomucoid- and ovalbumin-specific IgE/IgG(4) ratios in egg allergy. J Allergy Clin Immunol. 2012;129(3):739–47. [PubMed: 22277199]
28. Holt PG, Strickland D, Bosco A, Belgrave D, Hales B, Simpson A, et al. Distinguishing benign from pathologic TH2 immunity in atopic children. J Allergy Clin Immunol. 2016;137(2):379–87. [PubMed: 26518094]
29. Teng Y, Zhang R, Yu H, Wang H, Hong Z, Zhuang W, et al. Altered MicroRNA Expression Profiles in Activated Mast Cells Following IgE-FcepsilonRI Cross-Linking with Antigen. Cell Physiol Biochem. 2015;35(6):2098–110. [PubMed: 25895812]
30. Jayapal M, Tay HK, Reghunathan R, Zhi L, Chow KK, Rauff M, et al. Genome-wide gene expression profiling of human mast cells stimulated by IgE or FcepsilonRI-aggregation reveals a complex network of genes involved in inflammatory responses. BMC Genomics. 2006;7:210. [PubMed: 16911805]
31. Scholten J, Hartmann K, Gerbaulet A, Krieg T, Muller W, Testa G, et al. Mast cell-specific Cre/loxP-mediated recombination in vivo. Transgenic Res. 2008;17(2):307–15. [PubMed: 17972156]
32. Boross P, Breukel C, van Loo PF, van der Kaa J, Claassens JW, Bujard H, et al. Highly B lymphocyte-specific tamoxifen inducible transgene expression of CreER T2 by using the LC-1 locus BAC vector. Genesis. 2009;47(11):729–35. [PubMed: 19621440]
33. Burton OT, Darling AR, Zhou JS, Noval-Rivas M, Jones TG, Gurish MF, et al. Direct effects of IL-4 on mast cells drive their intestinal expansion and increase susceptibility to anaphylaxis in a murine model of food allergy. Mucosal Immunol. 2013;6(4):740–50. [PubMed: 23149659]
34. Derakhshan T, Samuchiwal SK, Hallen N, Bankova LG, Boyce JA, Barrett NA, et al. Lineage-specific regulation of inducible and constitutive mast cells in allergic airway inflammation. J Exp Med. 2021;218(1).
35. Love MI, Huber W, Anders S. Moderated estimation of fold change and dispersion for RNA-seq data with DESeq2. Genome Biol. 2014;15(12):550. [PubMed: 25516281]
36. Chen EY, Tan CM, Kou Y, Duan Q, Wang Z, Meirelles GV, et al. Enrichr: interactive and collaborative HTML5 gene list enrichment analysis tool. BMC Bioinformatics. 2013;14:128. [PubMed: 23586463]
37. Kuleshov MV, Jones MR, Rouillard AD, Fernandez NF, Duan Q, Wang Z, et al. Enrichr: a comprehensive gene set enrichment analysis web server 2016 update. Nucleic Acids Res. 2016;44(W1):W90–7. [PubMed: 27141961]
38. Xie Z, Bailey A, Kuleshov MV, Clarke DJB, Evangelista JE, Jenkins SL, et al. Gene Set Knowledge Discovery with Enrichr. Curr Protoc. 2021;1(3):e90. [PubMed: 33780170]
39. Liao S, Patil SU, Shreffler WG, Dreskin SC, Chen X. Human monoclonal antibodies to Ara h 2 inhibit allergen-induced, IgE-mediated cell activation. Clin Exp Allergy. 2019;49(8):1154–7. [PubMed: 31134696]
40. Combes AJ, Courau T, Kuhn NF, Hu KH, Ray A, Chen WS, et al. Global absence and targeting of protective immune states in severe COVID-19. Nature. 2021;591(7848):124–30. [PubMed: 33494096]
41. Takai T, Ono M, Hikida M, Ohmori H, Ravetch JV. Augmented humoral and anaphylactic responses in Fc gamma RII-deficient mice. Nature. 1996;379(6563):346–9. [PubMed: 8552190]
42. Wernersson S, Karlsson MC, Dahlstrom J, Mattsson R, Verbeek JS, Heyman B. IgG-mediated enhancement of antibody responses is low in Fc receptor gamma chain-deficient mice and increased in Fc gamma RII-deficient mice. J Immunol. 1999;163(2):618–22. [PubMed: 10395649]
43. Barrington RA, Pozdnyakova O, Zafari MR, Benjamin CD, Carroll MC. B lymphocyte memory: role of stromal cell complement and FcgammaRIIB receptors. J Exp Med. 2002;196(9):1189–99. [PubMed: 12417629]
44. Paul E, Nelde A, Verschoor A, Carroll MC. Follicular exclusion of autoreactive B cells requires FcgammaRIIb. Int Immunol. 2007;19(4):365–73. [PubMed: 17307801]

45. Boross P, Arandhara VL, Martin-Ramirez J, Santiago-Raber ML, Carlucci F, Flierman R, et al. The inhibiting Fc receptor for IgG, FcgammaRIIB, is a modifier of autoimmune susceptibility. J Immunol. 2011;187(3):1304–13. [PubMed: 21724994]
46. Chhiba KD, Hsu CL, Berdnikovs S, Bryce PJ. Transcriptional Heterogeneity of Mast Cells and Basophils upon Activation. J Immunol. 2017;198(12):4868–78. [PubMed: 28476932]
47. Siraganian RP, de Castro RO, Barbu EA, Zhang J. Mast cell signaling: the role of protein tyrosine kinase Syk, its activation and screening methods for new pathway participants. FEBS Lett. 2010;584(24):4933–40. [PubMed: 20696166]
48. Orengo JM, Radin AR, Kamat V, Badithe A, Ben LH, Bennett BL, et al. Treating cat allergy with monoclonal IgG antibodies that bind allergen and prevent IgE engagement. Nat Commun. 2018;9(1):1421. [PubMed: 29650949]
49. Asai K, Kitaura J, Kawakami Y, Yamagata N, Tsai M, Carbone DP, et al. Regulation of mast cell survival by IgE. Immunity. 2001;14(6):791–800. [PubMed: 11420048]
50. Mukai K, Tsai M, Saito H, Galli SJ. Mast cells as sources of cytokines, chemokines, and growth factors. Immunol Rev. 2018;282(1):121–50. [PubMed: 29431212]
51. Malbec O, Fong DC, Turner M, Tybulewicz VL, Cambier JC, Fridman WH, et al. Fc epsilon receptor I-associated lyn-dependent phosphorylation of Fc gamma receptor IIB during negative regulation of mast cell activation. J Immunol. 1998;160(4):1647–58. [PubMed: 9469421]
52. Nakata K, Yoshimaru T, Suzuki Y, Inoue T, Ra C, Yakura H, et al. Positive and negative regulation of high affinity IgE receptor signaling by Src homology region 2 domain-containing phosphatase 1. J Immunol. 2008;181(8):5414–24. [PubMed: 18832698]
53. Xie ZH, Zhang J, Siraganian RP. Positive regulation of c-Jun N-terminal kinase and TNF-alpha production but not histamine release by SHP-1 in RBL-2H3 mast cells. J Immunol. 2000;164(3):1521–8. [PubMed: 10640770]
54. Damen JE, Ware MD, Kalesnikoff J, Hughes MR, Krystal G. SHIP's C-terminus is essential for its hydrolysis of PIP3 and inhibition of mast cell degranulation. Blood. 2001;97(5):1343–51. [PubMed: 11222379]
55. Ujike A, Ishikawa Y, Ono M, Yuasa T, Yoshino T, Fukumoto M, et al. Modulation of immunoglobulin (Ig)E-mediated systemic anaphylaxis by low-affinity Fc receptors for IgG. J Exp Med. 1999;189(10):1573–9. [PubMed: 10330436]
56. Strait RT, Morris SC, Finkelman FD. IgG-blocking antibodies inhibit IgE-mediated anaphylaxis in vivo through both antigen interception and Fc gamma RIIb cross-linking. J Clin Invest. 2006;116(3):833–41. [PubMed: 16498503]
57. Shelburne CP, McCoy ME, Piekorz R, Sexl V, Roh KH, Jacobs-Helber SM, et al. Stat5 expression is critical for mast cell development and survival. Blood. 2003;102(4):1290–7. [PubMed: 12714518]
58. Ikeda K, Nakajima H, Suzuki K, Watanabe N, Kagami S, Iwamoto I. Stat5a is essential for the proliferation and survival of murine mast cells. Int Arch Allergy Immunol. 2005;137 Suppl 1:45–50.
59. Barnstein BO, Li G, Wang Z, Kennedy S, Chalfant C, Nakajima H, et al. Stat5 expression is required for IgE-mediated mast cell function. J Immunol. 2006;177(5):3421–6. [PubMed: 16920984]
60. Pullen NA, Barnstein BO, Falanga YT, Wang Z, Suzuki R, Tamang TD, et al. Novel mechanism for Fc{epsilon}RI-mediated signal transducer and activator of transcription 5 (STAT5) tyrosine phosphorylation and the selective influence of STAT5B over mast cell cytokine production. J Biol Chem. 2012;287(3):2045–54. [PubMed: 22130676]
61. Li G, Miskimen KL, Wang Z, Xie XY, Brenzovich J, Ryan JJ, et al. STAT5 requires the N-domain for suppression of miR15/16, induction of bcl-2, and survival signaling in myeloproliferative disease. Blood. 2010;115(7):1416–24. [PubMed: 20008792]
62. Gevaert P, De Craemer J, De Ruyck N, Rottey S, de Hoon J, Hellings PW, et al. Novel antibody cocktail targeting Bet v 1 rapidly and sustainably treats birch allergy symptoms in a phase 1 study. J Allergy Clin Immunol. 2022;149(1):189–99. [PubMed: 34126156]

Key Messages

- IgG-mediated inhibition of mast cell activation can occur either via epitope masking or by negative signaling via FcγRIIb. We demonstrate that receptor-mediated inhibition is significantly more sensitive.
- RNA sequencing reveals that IgE-dependent mast cell activation modulates the expression of 879 genes. Inhibitory IgG:FcγRIIb signaling impacts only 12% of these genes, many involved in driving type 2 inflammation. In contrast, STAT5a phosphorylation and downstream targets involved in mast cell survival are induced by IgE:FcεRI but unaffected by IgG:FcγRIIb.

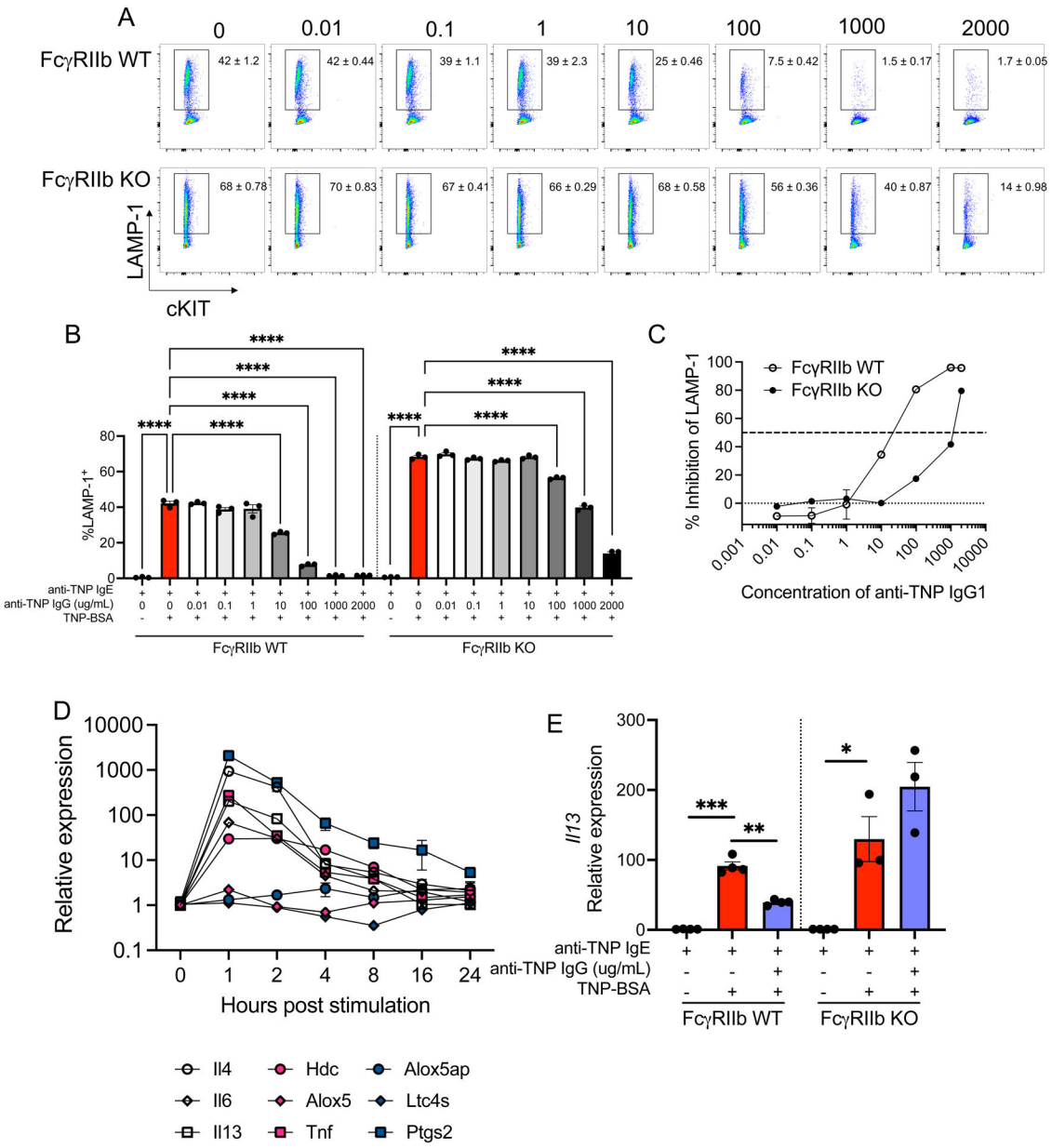

Figure 1: FcγRIIb-mediated antigen-specific IgG effects on mast cell activation

A) Representative dot plots of LAMP-1 expression by WT and FcγRIIb KO BMMCs. B) Bar plots for LAMP-1 expression by WT and FcγRIIb KO BMMCs following sensitization with 50 ng/mL anti-TNP IgE, treatment with varying concentrations of anti-TNP IgG and challenge with 50 ng/mL TNP-BSA for 10 minutes. C) Percent inhibition of LAMP-1 by anti-TNP IgG in both WT and FcγRIIb KO BMMCs sensitized with anti-TNP IgE and activated with TNP-BSA. Statistical significance represents comparisons between WT and KO cells at different doses of IgG1. D) mRNA expression time course for *Il4*, *Il6*, *Il13* and *TNFa* in WT BMMCs sensitized with 50 ng/mL anti-TNP IgE and activated with 50 ng/mL TNP-BSA. E) Expression of *Il13* in WT and KO BMMCs sensitized with 50 ng/mL anti-TNP IgE and degranulated with 50 ng/mL TNP-BSA in the presence or absence

of 10 μg/mL anti-TNP IgG. Data are shown for one experiment representative of n≥3 independent experiments with at least n=3 per group. Values are presented as means ± SEMs of independent replicates. *P<0.05, **P<0.01, ***P<0.001, and ****P<0.0001

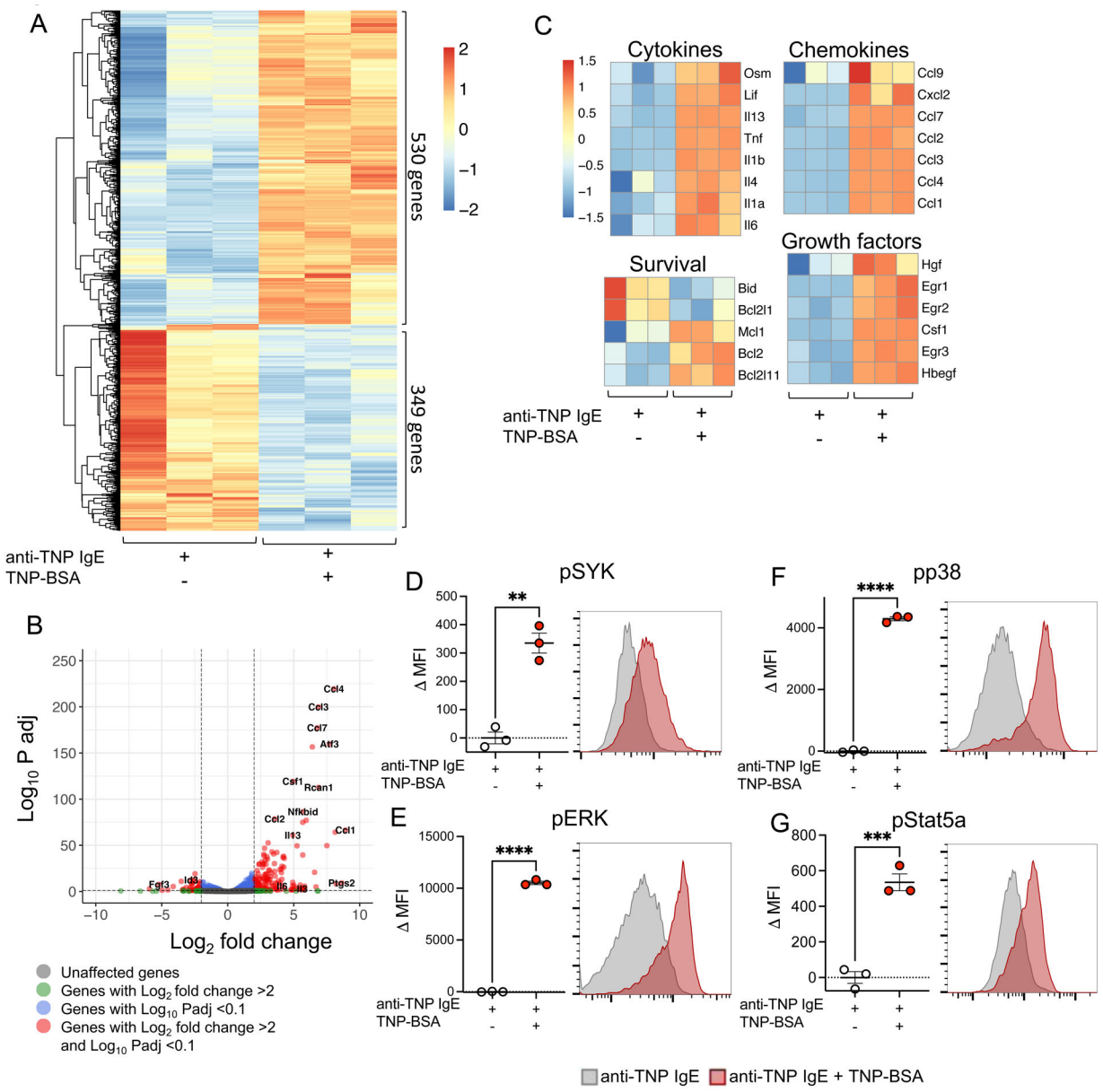

Figure 2: Effects of IgE-mediated activation on mast cell transcripts and pathways

A) Heatmap of transcripts differentially expressed between anti-TNP IgE-sensitized WT BMMCs that were either unchallenged or challenged with TNP-BSA (false discovery rate < 0.1, DeSeq2). B) Volcano plot indicating differentially expressed transcripts (false discovery rate < 0.1) between anti-TNP IgE-sensitized WT BMMCs that were either unchallenged or challenged with TNP-BSA, select genes are labelled. C) Heatmap of normalized counts of select genes clustering in “Cytokines”, “Chemokines”, “Survival” and “Growth factors” following IgE receptor crosslinking in WT BMMCs. D-G) Change in MFI and representative histograms depicting phosphorylation of D) SYK, E) ERK, F) p38 and G) Stat5a in WT BMMCs following IgE receptor crosslinking. Data are shown for one experiment representative of n≥3 independent experiments with at least n=3 per group.

Values are presented as means ± SEMs of independent replicates, scale bar indicates the z-score. ***P<0.001 and ****P<0.0001

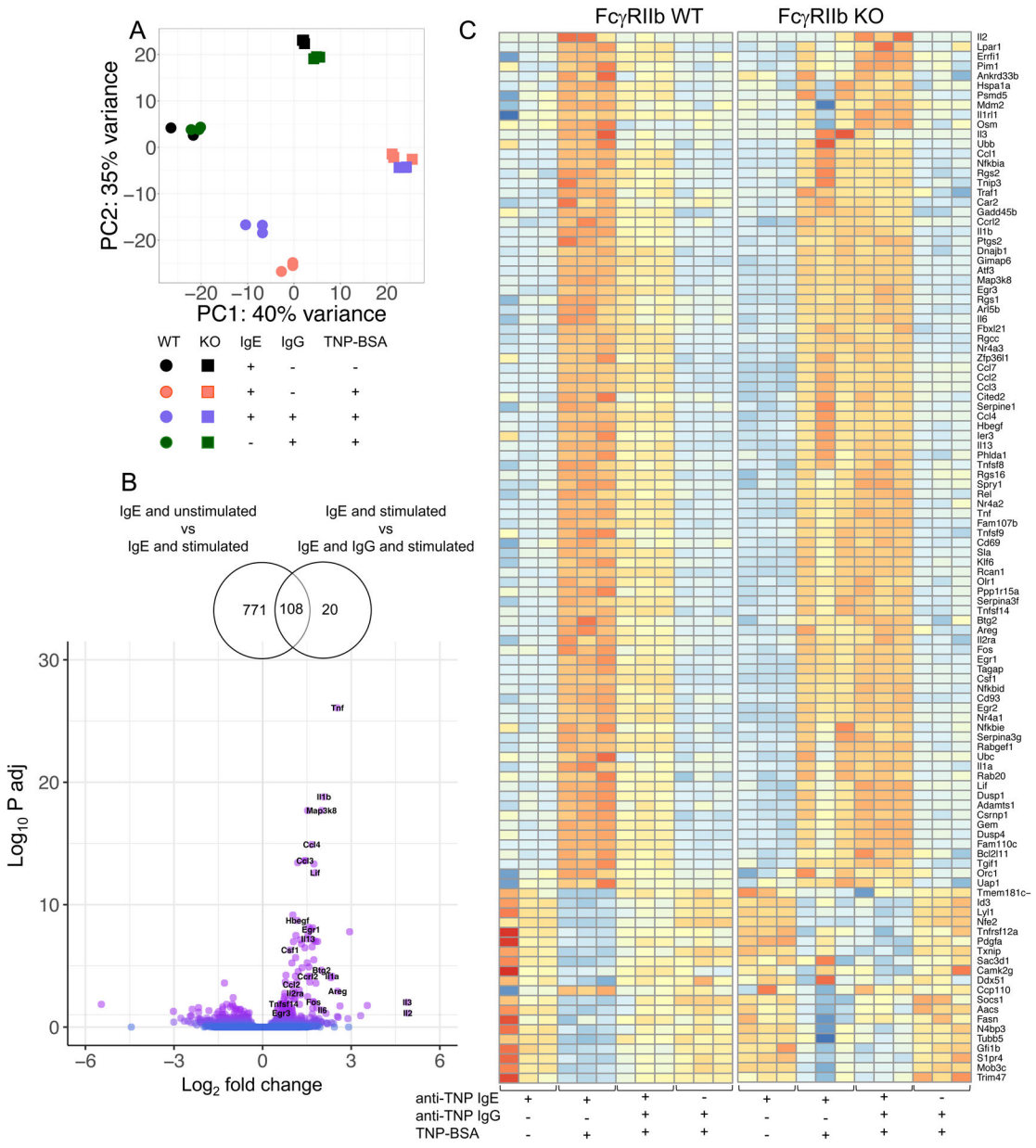

Figure 3: Identification of IgE-modulated transcripts and pathways that are altered in the presence of antigen-specific IgG

A) Principal component plot of WT and FcγRIIb KO BMMCs incubated with a combination of 50 ng/mL anti-TNP IgE and 10 μg/mL anti-TNP IgG. Reaction was stopped one hour after stimulation with or without 50 ng/mL TNP-BSA, and RNA was extracted. Percentages indicate the level of variance described by each component. Different colors represent different groups and n=3 per group. B) (Upper) Venn diagram representing number of genes changed by FcεRI crosslinking in WT cells (left circle) and number of genes changed by the presence of IgG during FcεRI crosslinking (right circle). (Lower) Volcano plot of genes significantly changed following FcεRI receptor crosslinking in the presence or absence of anti-TNP IgG. C) Heatmap of the 108 genes significantly changed when

comparing IgE-sensitized and TNP-BSA stimulated cells in the presence or absence of antigen-specific IgG (left). Representation of the same 108 genes in KO cells (right).

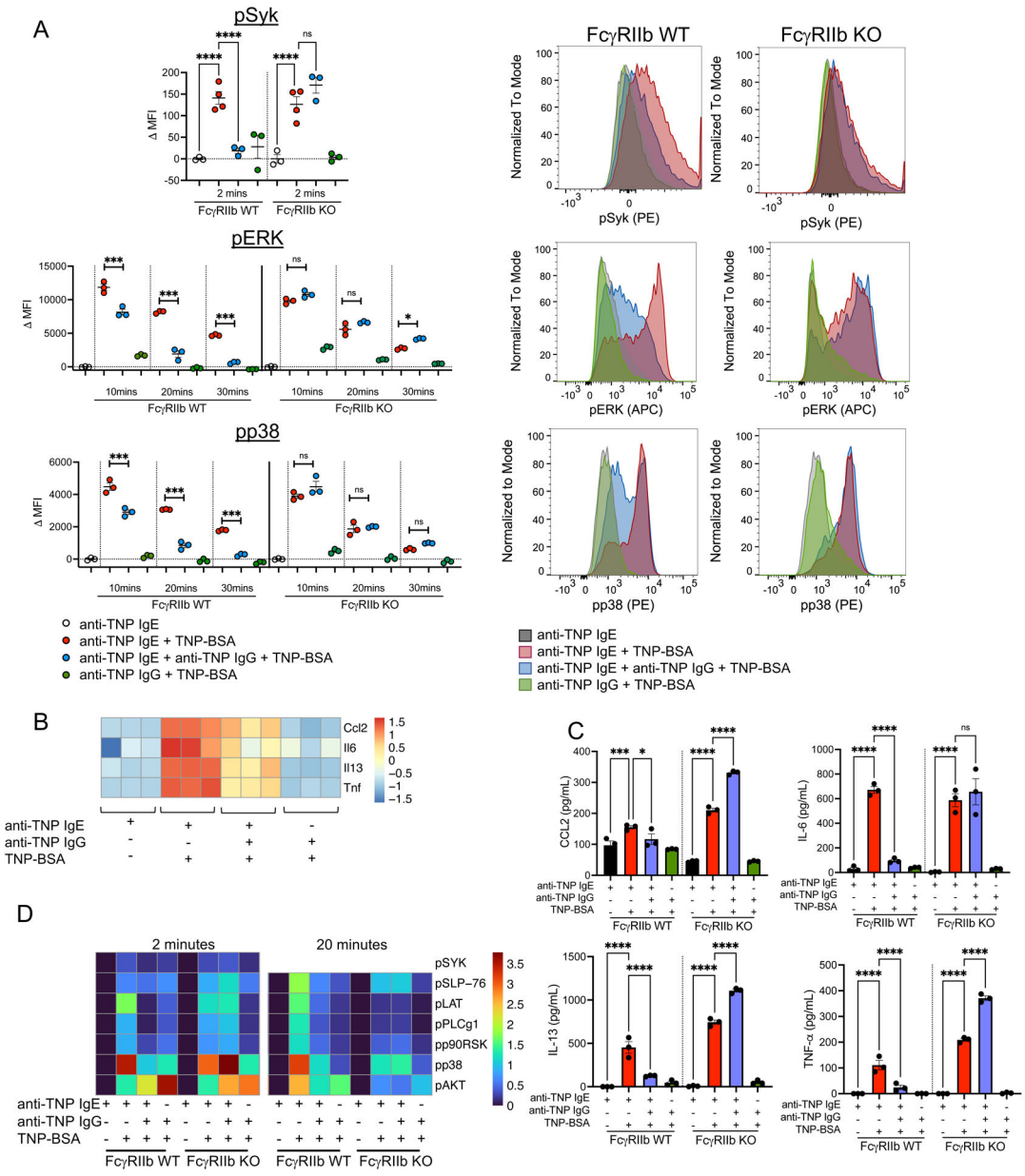

Figure 4: Role of FcγRIIb in IgG-mediated suppression of phosphorylation of SYK, ERK and p38, and secretion of cytokines and chemokines induced by IgE crosslinking

A) Histograms and dot plots of the MFI of phosphorylated forms of SYK (upper), ERK (middle) and p38 (lower) in WT and KO BMMCs following FcεRI crosslinking with 50 ng/mL TNP-BSA after sensitization with 50 ng/mL anti-TNP IgE in the presence or absence of antigen-specific IgG (10 μg/mL). B) Heatmap of cytokines and chemokines significantly changed by the presence of antigen-specific IgG during antigen-specific IgE receptor crosslinking in WT BMMCs (left) and unaffected in FcγRIIb KO BMMCs. C) Secretion of CCL2, IL-6, IL-13 and TNF-a by WT and KO BMMCs following FcεRI crosslinking in the presence or absence of antigen-specific IgG. D) Heatmap of phosphorylation intensities for SYK and SYK related proteins at 2 and 20 minutes following IgE receptor crosslinking. Data are represented as unscaled values of the fold change in mean metal intensities (FC

in MMI) for each group relative to the sensitized only group within each strain. Data are shown for one experiment representative of n≥2 independent experiments with at least n=3 per group. For dot plots, values are presented as means ± SEMs of independent replicates. *P<0.05, **P<0.01, ***P<0.001, and ****P<0.0001

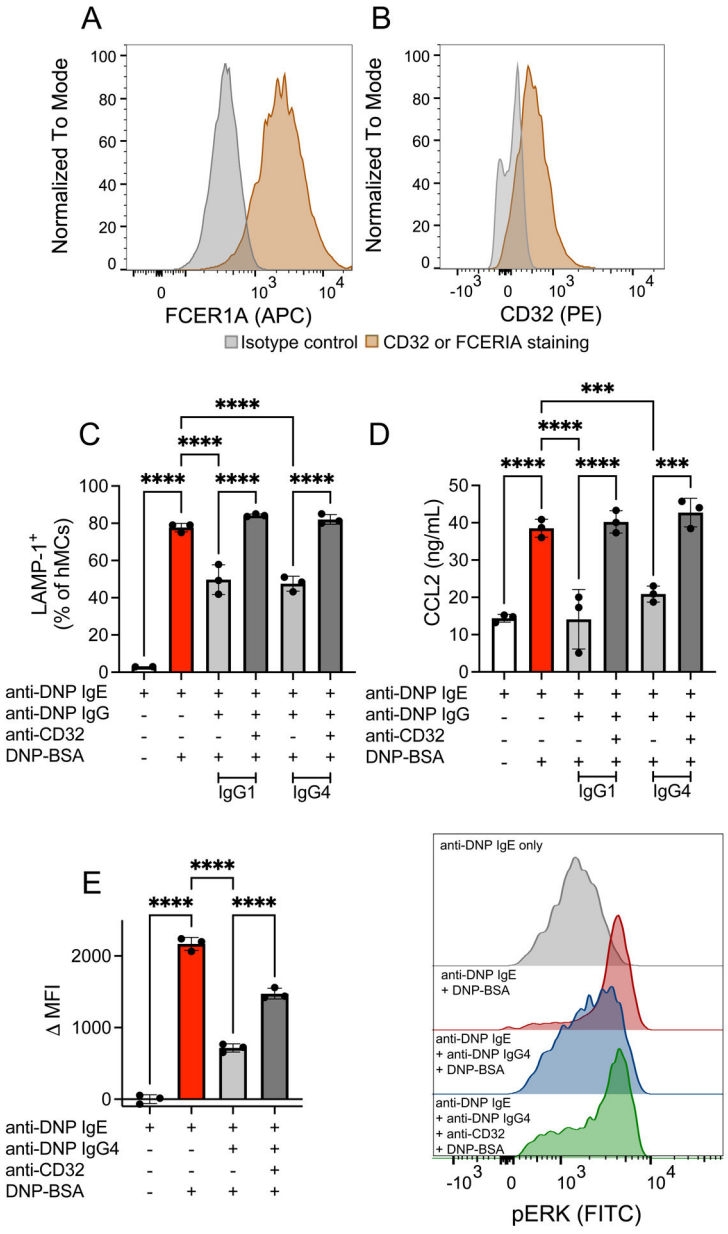

Figure 5: CD32-mediated effects of antigen-specific IgG on human mast cell activation

Histograms representing the surface expression of FcεRI (A) and CD32 (B) on human peripheral blood derived MCs (hMCs). Bar plots representing LAMP-1^{+} upregulation (C) or CCL2 secretion (D) by hMCs sensitized with anti-DNP IgE and treated with either 30 μg/mL anti-DNP IgG1 or anti-DNP IgG4. For some conditions, cells were pre-incubated with 2 μg anti-CD32 prior to the addition of IgG. Cells were stimulated with 50 ng/mL DNP-BSA. E) Bar plots and histograms representing the phosphorylation of ERK in anti-DNP IgE-sensitized hMCs stimulated with DNP-BSA in the presence or absence of anti-DNP IgG4 and anti CD32. Data are shown for one experiment representative of n≥3 independent experiments with at least n=3 per group. Values are presented as means ± SEMs of independent replicates. ***P<0.001 and ****P<0.0001

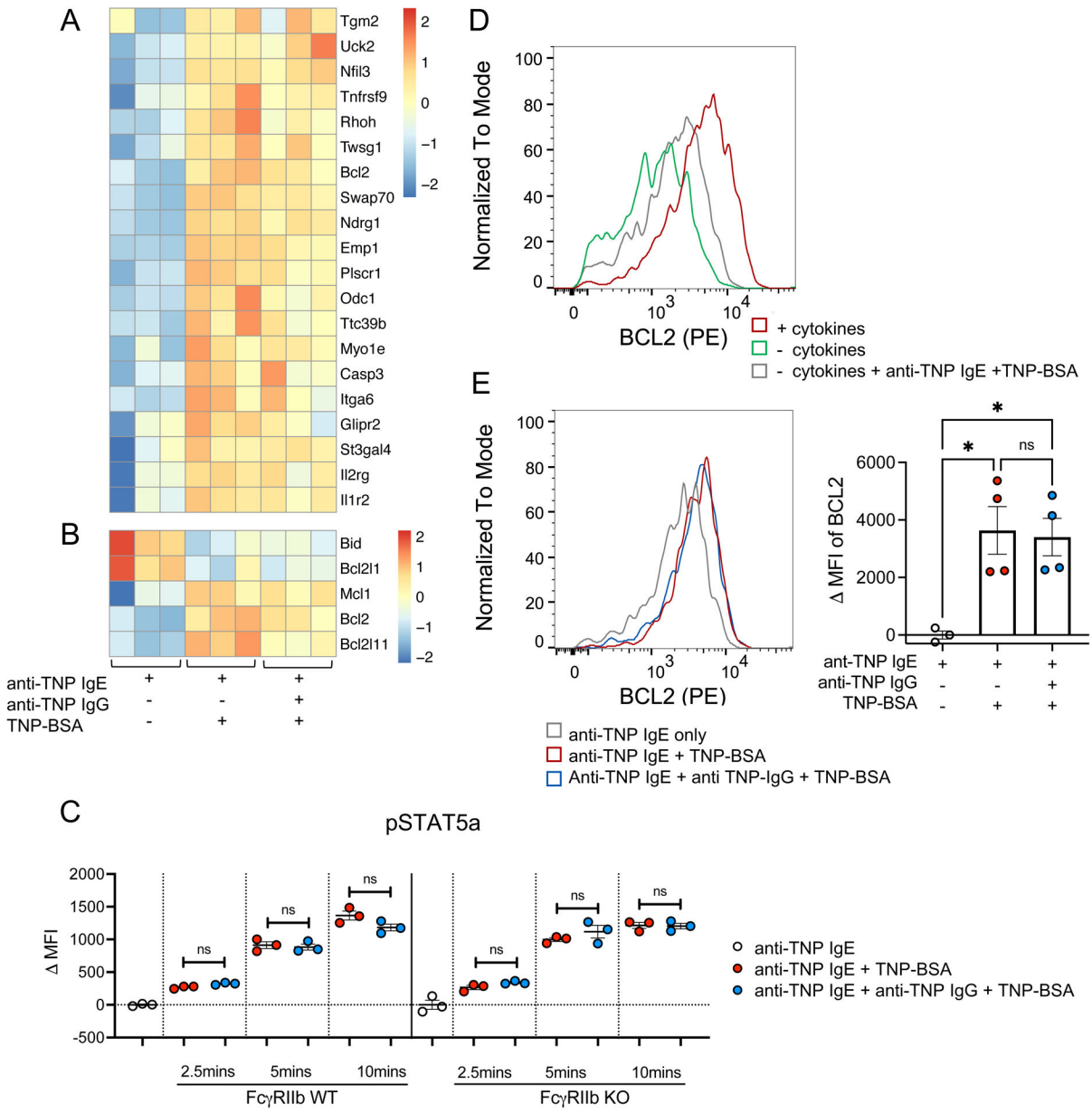

Figure 6: Lack of antigen-specific IgG effects on the phosphorylation of STAT5a or changes in STAT5a-associated transcripts in IgE-activated BMMCs

Heatmaps of change in expression of Stat5a associated transcripts (A) and survival associated genes (B) in WT cells. C) Time course of the phosphorylation of Stat5a in WT and FcγRIIb KO cells following IgE receptor crosslinking (50 ng/mL of anti-TNP IgE and 50 ng/mL of TNP-BSA) in the presence or absence of antigen-specific IgG (10 μg/mL). D) Histogram representing changes in BCL-2 expression following cytokine deprivation or IgE receptor crosslinking. E) Change in BCL-2 expression following IgE receptor crosslinking in the presence or absence of allergen specific IgG. Data are shown for one experiment representative of n≥3 independent experiments with at least n=3 per group. Values are presented as means ± SEMs of independent replicates. *P<0.05

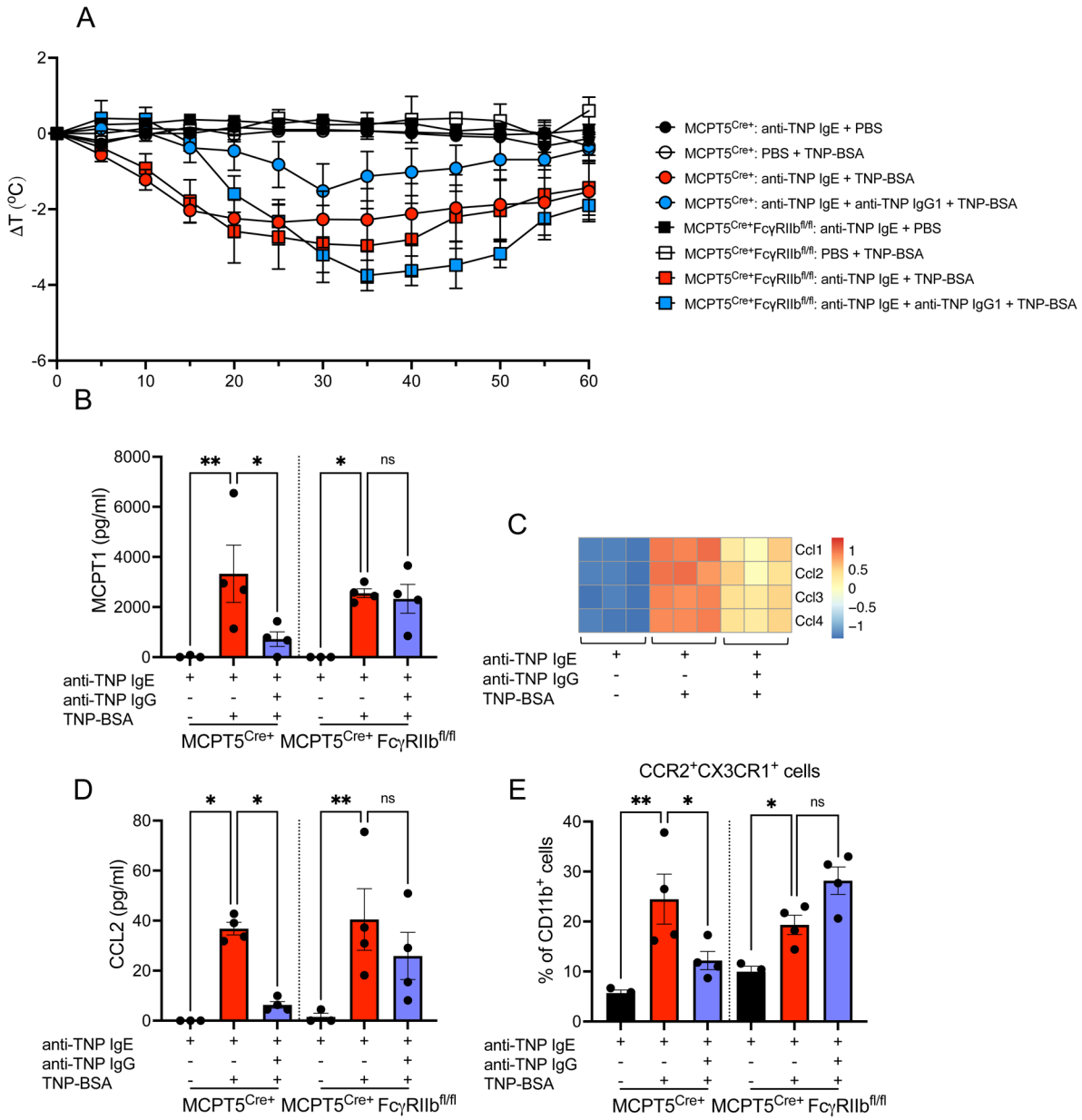

Figure 7: Antigen-specific IgG effects on IgE-mediated anaphylaxis and the recruitment of inflammatory cells.

A) Change in core body temperature in Mcpt5Cre^{+} and Mcpt5Cre^{+}FcγRIIb$^{fl/fl}$ sensitized with 2 μg anti-TNP IgE in the presence or absence of 100 μg anti-TNP IgG and challenged with 100 μg of TNP-BSA. B) Serum levels of mouse MC protease 1 (MCPT1) collected two hours following induction of anaphylaxis. C) Heatmap representing changes in chemokine transcript expression following IgE receptor crosslinking in the presence or absence of antigen-specific IgG. D) Concentration of CCL2 in the peritoneal lavage six hours after the induction of anaphylaxis. E) Recruitment of inflammatory monocytes to the peritoneal space six hours following the induction of anaphylaxis. Data are shown for one experiment representative of n≥2 independent experiments with at least n=3 per group. Values are presented as means ± SEMs of independent replicates. *P<0.05 and **P<0.01. Results from

multiple paired comparisons between individual groups by two-way ANOVA are presented in Table S4.